Accurate Susceptibility Quantification from MR Phase Data through the Least Squares Fit Method: Phantom Validation

J. Neelavalli[1,2], Y-C. N. Cheng[3], M. Kamran[2], J. V. Byrne[2], and E. M. Haacke[3]
[1]The MRI Institute for Biomedical Research, Detroit, Michigan, United States, [2]Nuffield Department of Surgery, University of Oxford, Oxford, Oxfordshire, United Kingdom, [3]Academic Radiology, Wayne State University, Detroit, Michigan, United States

Introduction: Quantifying magnetic susceptibility of biological tissue using MRI has important clinical implications such as quantifying iron deposition in liver and sub-cortical structures, measuring oxygen saturation in blood, differentiating a hemorrhagic lesion as acute or chronic and identifying calcifications etc.. MR susceptometry of substances taken in standard sphere or cylinder geometries has been done in the past [1,2] through a straight forward field fitting approach. Previously we had evaluated a 3D least-squares algorithm for susceptibility quantification of a single arbitrarily shaped object [4]. This algorithm was based on the Fourier based method for calculating field perturbation from an arbitrary susceptibility distribution. Here we extend this quantification work to a multiple susceptibility-component model. In addition, we apply the method here on a very small object occupying only a few pixels to understand the affect of discretization.

Materials and Methods: A phantom with a relatively complicated shape, containing 10mM gadolinium solution in a test tube and distilled water in two different compartments, was constructed (Fig. 1) and imaged at 3.0T on Siemens Trio scanner. The middle dark spot in Fig. 1 is the air pocket at the end of the gadolinium tube. Gradient echo complex data were acquired using a circularly polarized head coil at TR 15 ms, FA 10º, BW 610Hz/pixel, echo times (TE) 6.61, and 8.11 msec with isotropic resolution of 0.75mm in a 256x256x192 matrix. Phase maps with effective echo time of 1.5msec were generated through complex dividing the two datasets. Before acquiring phase data, shimming was performed with a spherical phantom to 10Hz FWHM frequency dispersion. Magnitude images at echo time 6.61 msec were used to obtain geometries of the individual water and gadolinium compartments [6]. Algorithm detailed in [4] was used for susceptibility quantification. Only the central 128^3 volume (as shown in Fig. 3) was used for the fitting procedure. Initial values of -6 ppm and -2 ppm for water and gadolinium solution were used in the algorithm, respectively. In the quantification procedure, the quantified susceptibility values are relative to air. Theoretically expected absolute volume susceptibility for the gadolinium solution was calculated to be -5.65ppm relative to vacuum and -6.01ppm relative to air. This was based on the 0.5 M gadolinium solution that has a susceptibility value of approximately 170 ppm (SI units) [2]. In addition to the Green's function defined in [4], we also used Jenkinson et al.'s kernel defined in [3], without the suggested zero padding, for susceptibility quantifications and comparisons.

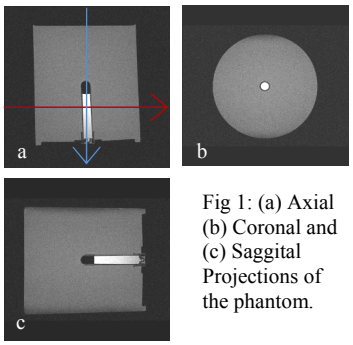

Fig 1: (a) Axial (b) Coronal and (c) Saggital Projections of the phantom.

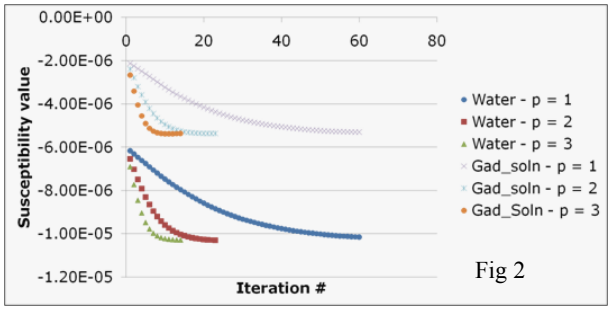

Fig 2

Table 1

Threshold value 'p'	*Gad-soln. (χ in ppm)*	*Water (χ in ppm)*	*chi-square per point*	*# of Iterations*
1	*-5.36 ± 0.0024*	*-10.28 ± 0.0044*	*0.327*	*60*
2	*-5.36 ± 0.002*	*-10.29 ± 0.003*	*1.24*	*23*
3	*-5.30 ± 0.0015*	*-10.15 ± 0.0026*	*2.56*	*14*

Results and Discussion: Figure 2 shows the convergence of the susceptibility values of gadolinium solution and water for different noise threshold values (i.e., p value of 3 includes more noise voxels than those from a p value of 1). Table 1 shows the quantified susceptibility values and their associated errors along with the corresponding goodness-of-fit parameter, chi-square/point. The algorithm converges to almost the same values irrespective of the p value used. However, with more stringent the p value, it takes more iterations for convergence. The converged χ values for water and gadolinium solution are roughly -10.3 ppm and -5.36 ppm respectively. These values deviate from the theoretical values of -9.4ppm for water and -6.01ppm for gadolinium solution by 10% and 11% respectively. Furthermore, the χ values obtained from Jenkinson et al.'s kernel agree well within 1% with those shown in Table 1. This indicates the equivalence of the Green's function in [4] to the kernel in [3]. Clearly from Table 1, the errors calculated from the least squares fit do not explain these large deviations of about 11%. The differences are likely due to the narrow diameter of the Gadolinium tube, which is 12 voxels wide. This lower resolution could lead to discretization error, i.e. improper representation of the small objects due to finite voxel sizes, which can lead to error in susceptibility quantification. Figure 3 shows the voxel-map which indicates the set of voxels used in quantification in the final iteration for p=2. We see that the voxels within and around the cylinder containing gad-soln. are only sparsely utilized possibly contributing to the quantification error. Furthermore, eddy-current effects could also cause phase corruption thus affecting quantification. Nonetheless, an absolute accuracy of within 11% is still valuable in biological setting [7].

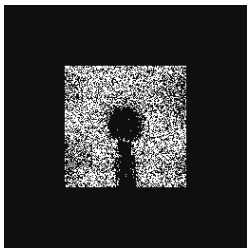

Fig 3: Map of voxels (white area) selected for susceptibility quantification in the final

Conclusion: The larger than expected errors are likely due to the pixelization in images. This problem was noted but its effect was not fully studied. Our work suggests that more studies should pay attention to medium size objects before this quantitative method is applied *in vivo*. As expected from the theoretical point of view, we show that this method is equivalent to the method used in [3].

References: [1] Chu, S.C., et al., Magn Reson Med, 1990. 13(2): p. 239-62. [2] Weisskoff, R.M., et.al. Magn Reson Med, 1992. 24(2): p. 375-83. [3] Jenkinson, M., et.al. Magn Reson Med, 2004. 52(3): p. 471-7. [4] Cheng, Y.C., et.al. Phys Med Biol, 2009. 54(5): p. 1169-89. [5] Maques JP et al Concepts in Magnetic Resonance B, 2005;25: 65-78..[6] Pandian DS et al JMRI 2008;28(3):727-735. [7] Haacke EM, Cheng YCN, et. al., Magn Reson Imaging. 2005; 23(1): 1-25.